Chirality-Controlling Chelate (CCC) Ligands in Analogues of Platinum Anticancer Agents. Influence of N9 Substituents of Guanine Derivatives (G) on the Distribution of Chiral Conformers of (CCC)PtG_2 with CCC = *N,N′*-Dimethyl-2,3-diaminobutane

Luigi G. Marzilli,*,† Francesco P. Intini,‡ Danita Kiser,† Hing C. Wong,† Susan O. Ano,† Patricia A. Marzilli,† and Giovanni Natile*,‡

Department of Chemistry, Emory University, Atlanta, Georgia 30322, and Dipartimento Farmaco-Chimico, Università degli Studi di Bari, 70125 Bari, Italy

Received July 21, 1998

Chirality-controlling chelate (**CCC**) ligands are a class of chiral diamine ligands with one or two chiral secondary amine ligating groups. Analogues of platinum anticancer agents containing **CCC** ligands exhibit unusual steric and dynamic features. In this study NMR and CD methods were used to evaluate the influence of the N9 substituent in guanine derivatives (**G**) on conformer distribution in one class of (**CCC**)Pt$\mathbf{G_2}$ complexes. We employed the **CCC** ligand, *N,N′*-dimethyl-2,3-diaminobutane [**Me_2DAB** with *S,R,R,S* or *R,S,S,R* configurations at the four asymmetric centers, N, C, C, and N]. For each **Me_2DAB**Pt$\mathbf{G}_2$ complex, the presence of four **G** H8 signals demonstrated formation of all three possible atropisomers: ΔHT (head-to-tail), ΛHT, and HH (head-to-head). Different **G** ligands (5′-GMP, 3′-GMP, 1-MeGuo, Guo, or 9-EtG) were chosen to assess the effect of the N9 substituent on the relative stability and spectral properties of the atropisomers. The conformations of the atropisomers of **Me_2DAB**Pt$\mathbf{G}_2$ were determined from CD spectra and from NOE cross-peaks (assigned via COSY spectra) between **G** H8 signals and those for the **Me_2DAB** protons. Regardless of the N9 substituent, the major form was HT. However, this form had the opposite chirality, ΛHT and ΔHT, and base tilt direction, left- and right-handed, respectively, for the *S,R,R,S* and *R,S,S,R* configurations of the **Me_2DAB** ligand. Thus, the chirality of the **CCC** ligand, not hydrogen bonding, is the most important determinant of conformation. For each **Me_2DAB**Pt$\mathbf{G}_2$ complex, the tilt direction of all three atropisomers is the same and, except for 5′-GMP, the order of abundance was major HT > minor HT > HH. For 5′-GMP, the HH atropisomer was three times as abundant as the minor HT species, suggesting that phosphate-NH(**Me_2DAB**) hydrogen bonds could be present since such bonding is possible only for the 5′-GMP derivatives. However, if such phosphate-NH hydrogen bonds exist, they are weak since the percentage of the major HT form of 5′-GMP complexes is similar and indeed can be smaller compared to this percentage for complexes with other **G**'s. The CD spectra of all (*S,R,R,S*)-**Me_2DAB**Pt$\mathbf{G}_2$ complexes were similar and opposite to those of all (*R,S,S,R*)-**Me_2DAB**Pt$\mathbf{G}_2$ complexes, indicating the CD signature is characteristic of the dominant HT conformer, which has a chirality dictated by the chirality of the **CCC** ligand and not the N9 substituent.

Introduction

The anticancer drug, *cis*-$PtCl_2(NH_3)_2$ (cisplatin), and its less nephrotoxic derivative, carboplatin, are among the most effective anticancer agents known. The precise mechanism of action is not completely understood, but it is known that the drugs primarily target nuclear DNA, forming a critical lesion by cross-linking two adjacent guanine bases or an adenine and a guanine base via two Pt−N7 bonds.[1,2] Although a large number of cisplatin analogues, *cis*-PtX_2A_2 (A_2 = two unidentate or one bidentate amine ligand), are active, those with A_2 = tertiary amines are less active.[2,3] This observation has led to much speculation regarding the role of the amine protons[3−9] and to a number of studies of *cis*-$PtA_2\mathbf{G}_2$ (**G** = a guanine derivative) cross-link models reviewed briefly in the following paragraphs (all Pt**G** complexes mentioned here have Pt−N7 bonds).

It has been proposed that the coordinated NH forms intramolecular hydrogen bond(s) with the **G** O6[9−12] and/or a phosphate oxygen,[4,5,8,13−18] thereby enhancing the formation of a distorted

† Emory University.
‡ Università degli Studi di Bari.

(1) Reedijk, J. *J. Chem. Soc., Chem. Commun.* **1996**, 801.
(2) Sundquist, W. I.; Lippard, S. J. *Coord. Chem. Rev.* **1990**, *100*, 293.
(3) Johnson, N. P.; Butour, J.; Villani, G.; Wimmer, F. L.; Defais, M.; Pierson, V.; Brabec, V. *Prog. Clin. Biochem. Med.* **1989**, *10*, 1.
(4) Berners-Price, S. J.; Frey, U.; Ranford, J. D.; Sadler, P. J. *J. Am. Chem. Soc.* **1993**, *115*, 8649.
(5) Fouts, C. S.; Marzilli, L. G.; Byrd, R. A.; Summers, M. F.; Zon, G.; Shinozuka, K. *Inorg. Chem.* **1988**, *27*, 366.
(6) Kiser, D.; Intini, F. P.; Xu, Y.; Natile, G.; Marzilli, L. G. *Inorg. Chem.* **1994**, *33*, 4149.
(7) Reily, M. D.; Wilkowski, K.; Shinozuka, K.; Marzilli, L. G. *Inorg. Chem.* **1985**, *24*, 37.
(8) Reedijk, J. *Inorg. Chim. Acta* **1992**, *198−200*, 873.
(9) Xu, Y.; Natile, G.; Intini, F. P.; Marzilli, L. G. *J. Am. Chem. Soc.* **1990**, *112*, 8177.
(10) Sherman, S. E.; Gibson, D.; Wang, A. H. J.; Lippard, S. J. *J. Am. Chem. Soc.* **1988**, *110*, 7368.
(11) Hambley, T. W. *Inorg. Chem.* **1988**, *27*, 1073.
(12) Admiraal, G.; Van der Veer, J. L.; de Graaff, R. A. G.; den Hartog, J. H. J.; Reedijk, J. *J. Am. Chem. Soc.* **1987**, *109*, 592.
(13) Kozelka, J.; Petsko, G. A.; Lippard, S. J.; Quigley, G. J. *J. Am. Chem. Soc.* **1985**, *107*, 4079.
(14) Sherman, S. E.; Gibson, D.; Wang, A. H.; Lippard, S. J. *Science* **1985**, *230*, 412.
(15) den Hartog, J. H. J.; Altona, C.; van der Marel, G. A.; Reedijk, J. *Eur. J. Biochem.* **1985**, *147*, 371.

10.1021/ic980843f CCC: $15.00
Published on Web 12/01/1998

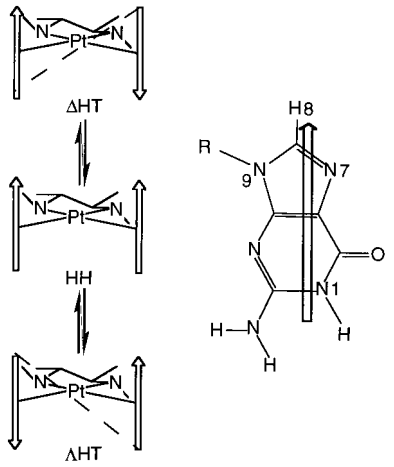

Figure 1. Depiction of **Me$_2$DAB**Pt**G**$_2$ conformers. Arrows represent a N7-bound **G**, where the arrowheads are H8 atoms; the definition of the ΔHT and ΛHT chirality is described in the text.

Pt−DNA adduct.[8,16] The existence of both types of intramolecular phosphate−NH and O6−NH hydrogen bonds in some *cis*-PtA$_2$**G**$_2$ adducts has been demonstrated in the solid state[10,14,19−21] and supported by modeling calculations.[11,13,22−24] Downfield-shifted ^{31}P,[5,15,16,23] ^{15}N,[4,17] or certain ^{1}H[4,6,15,17,18,25] NMR signals have been interpreted as indications of phosphate−NH or O6−NH hydrogen bonding. Downfield-shifting of one NH ^{1}H NMR signal at pH values around the phosphate pK_a was attributed to phosphate−NH hydrogen bonding.[4,18,25]

All published studies of oligonucleotides have suggested that the two adjacent cross-linked **G**'s favor the head-to-head (HH) conformation with both H8's on the same side of the platinum coordination plane (Figure 1).[5,10,12,17,26−28] In DNA and oligonucleotide duplexes, such cross-links are restricted by the phosphodiester linkage and GC Watson−Crick base pairing to the HH conformation.[29−32] Molecular mechanics calculations,[24] NMR evidence,[33] and X-ray data[12,34] suggest that the dihedral angles of the guanine planes with respect to the coordination plane are quite variable in HH conformers. In one case, a highly distorted structure, with one guanine base oriented nearly perpendicular to the other, was found.[33] In this adduct, one **G** residue was syn, whereas in most typical adducts both **G** residues are anti.[35]

In *cis*-PtA$_2$**G**$_2$ complexes, where the two **G**'s are not tethered, the head-to-tail (HT) atropisomers (Figure 1) are normally believed to dominate.[35] When A is a primary amine or NH$_3$, interconversion of all atropisomers by the **G**'s rotating around the Pt−N7 bonds is fast on the NMR time scale. When the *cis*-PtA$_2$ moiety is C_2 symmetric, a single **G** H8 NMR signal is observed; this signal is thought to reflect the average of all possible nucleotide orientations, with the HT forms dominating.[36−40] Restricted rotation has been demonstrated when Pt binds to adenine derivatives,[41] and it was possible to demonstrate in such cases that the HT forms do dominate; later, NMR data were used to estimate that the Pt−N7 rotation barrier is ∼50 kJ/mol lower for *cis*-Pt(NH$_3$)$_2$(5′-GMP)$_2$ than for *cis*-Pt(NH$_3$)$_2$(5′-AMP)$_2$.[42,43]

It is generally assumed that HH forms are dominant in the oligonucleotides because of the tether and that these HH forms do not undergo the dynamic motion observed for the untethered models. However, NMR methods cannot easily differentiate between the case of one conformer in a relatively fixed state and the case of a mixture of conformers in rapid dynamic motion, a limitation we refer to as the dynamic motion problem. It is ironic that the same type of data, the observation of one signal for a given type of proton, leads to quite different conclusions in the literature.[35]

Use of Pt compounds with bulky A$_2$ ligands can greatly diminish dynamic motion.[6,9,35−38,44] In recent studies of *cis*-PtA$_2$(d(GpG)) adducts in which A$_2$ is a chiral, bulky, diamine ligand, we have identified several new rotamers, including a second d(GpG) HH adduct without syn residues and an HT adduct.[45] In one such case, the HT rotamer has comparable stability to the HH rotamer.[46] The main reason that HT rotamers were presumed not to be favored for **G**'s connected with a sugar−phosphate−sugar linkage was the failure to observe such forms. However, failure to observe any HT form for *cis*-Pt(NH$_3$)$_2$(d(GpG)) may well be the result of the dynamic motion problem, not the result of the low stability of such HT forms.

For simpler *cis*-PtA$_2$**G**$_2$ complexes, evidence for multiple atropisomers can be observed most easily through the detection of more than one **G** H8 NMR signal when Pt−N7 bond rotation is slowed by a bulky A$_2$ ligand.[36,38] Early NMR studies attributed multiple H8 signals to HT atropisomers.[36,38,41] In solution, H8

(16) Bloemink, M. J.; Heetebrij, R. J.; Inagaki, K.; Kidani, Y.; Reedijk, J. *Inorg. Chem.* **1992**, *31*, 4656.
(17) Berners-Price, S. J.; Frenkiel, T. A.; Ranford, J. D.; Sadler, P. J. *J. Chem. Soc., Dalton Trans.* **1992**, 2137.
(18) Berners-Price, S. J.; Ranford, J. D.; Sadler, P. J. *Inorg. Chem.* **1994**, *33*, 5842.
(19) Gellert, R. W.; Bau, R. *J. Am. Chem. Soc.* **1975**, *97*, 7379.
(20) Lippert, B. *Prog. Inorg. Chem.* **1989**, *37*, 1.
(21) Admiraal, G.; Alink, M.; Altona, C.; Dijt, F. J.; van Garderen, C. J.; de Graaff, R. A. G.; Reedijk, J. *J. Am. Chem. Soc.* **1992**, *114*, 930.
(22) Hambley, T. W. *Inorg. Chem.* **1991**, *30*, 937.
(23) Herman, F.; Kozelka, J.; Stoven, V.; Guittet, E.; Girault, J.; Huynh-Dinh, T.; Igolen, J.; Lallemand, J.; Chottard, J. *Eur. J. Biochem.* **1990**, *194*, 119.
(24) Yao, S. J.; Plastaras, J. P.; Marzilli, L. G. *Inorg. Chem.* **1994**, *33*, 6061.
(25) Guo, Z.; Sadler, P. J.; Zang, E. *J. Chem. Soc., Chem. Commun.* **1997**, 27.
(26) Kline, T. P.; Marzilli, L. G.; Live, D.; Zon, G. *J. Am. Chem. Soc.* **1989**, *111*, 7057.
(27) Mukundan, S., Jr.; Xu, Y.; Zon, G.; Marzilli, L. G. *J. Am. Chem. Soc.* **1991**, *113*, 3021.
(28) Neumann, J.; Tran-Dinh, S.; Girault, J.; Chottard, J.; Huynh-Dinh, T. *Eur. J. Biochem.* **1984**, *141*, 465.
(29) Takahara, P. M.; Rosenzweig, A. C.; Frederick, C. A.; Lippard, S. J. *Nature* **1995**, *377*, 649.
(30) Takahara, P. M.; Frederick, C. A.; Lippard, S. J. *J. Am. Chem. Soc.* **1996**, *118*, 12309.
(31) Yang, D.; van Boom, S. S. G. E.; Reedijk, J.; van Boom, J. H.; Wang, A. H.-J. *Biochemistry* **1995**, *34*, 12912.
(32) van Boom, S. S. G. E.; Yang, D.; Reedijk, J.; van der Marel, G. A.; Wang, A. H.-J. *J. Biomol. Struct. Dyn.* **1996**, *13*, 989.
(33) Iwamoto, M.; Mukundan, S., Jr.; Marzilli, L. G. *J. Am. Chem. Soc.* **1994**, *116*, 6238.
(34) Lippert, B.; Raudaschl-Sieber, G.; Lock, C. J. L.; Pilon, P. *Inorg. Chim. Acta* **1984**, *93*, 43.
(35) Ano, S. O.; Kuklenyik, Z.; Marzilli, L. G. In *30 Years of Cisplatin: Chemistry and Biochemistry of a Leading Anticancer Drug*; Lippert, B., Ed.; Wiley-VCH: Basel, in press.
(36) Cramer, R. E.; Dahlstrom, P. L. *J. Am. Chem. Soc.* **1979**, *101*, 3679.
(37) Cramer, R. E.; Dahlstrom, P. L.; Seu, M. J. T.; Norton, T.; Kashiwagi, M. *Inorg. Chem.* **1980**, *19*, 148.
(38) Cramer, R. E.; Dahlstrom, P. L. *Inorg. Chem.* **1985**, *24*, 3420.
(39) Dijt, F. J.; Canters, G. W.; den Hartog, J. H. J.; Marcelis, A. T. M.; Reedijk, J. *J. Am. Chem. Soc.* **1984**, *106*, 3644.
(40) Miller, S. K.; Marzilli, L. G. *Inorg. Chem.* **1985**, *24*, 2421.
(41) Reily, M. D.; Marzilli, L. G. *J. Am. Chem. Soc.* **1986**, *108*, 6785.
(42) Li, D.; Bose, R. N. *J. Chem. Soc., Chem. Commun.* **1992**, 1596.
(43) Li, D.; Bose, R. N. *J. Chem. Soc., Dalton Trans.* **1994**, 3717.
(44) Ano, S. O.; Intini, F. P.; Natile, G.; Marzilli, L. G. *J. Am. Chem. Soc.* **1997**, *119*, 8570.
(45) Ano, S. O.; Intini, F. P.; Natile, G.; Marzilli, L. G. *J. Am. Chem. Soc.* **1998**, in press.
(46) Ano, S. O.; Intini, F. P.; Natile, G.; Marzilli, L. G., manuscript in preparation.

Chart 1. Sketches of the (*S,R,R,S*)- and (*R,S,S,R*)-**Me$_2$DAB**Pt Moieties

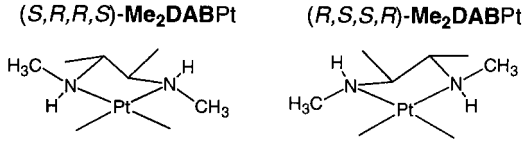

signals consistent with HH atropisomers of *cis*-PtA_2**G**$_2$ complexes have rarely been reported and only recently.[6,9,44]

The HH form was first clearly established for a *cis*-PtA_2**G**$_2$ system with the bulky, C_2-symmetrical **Me$_2$DAB** (*N,N*′-dimethyl-2,3-diaminobutane) ligand, (*S,R,R,S*)-**Me$_2$DAB** (where the configurations at the four asymmetric centers are *S, R, R,* and *S* at N, C, C, and N, respectively) (Chart 1). The structures are presented with the square plane of the platinum complex perpendicular to the plane of the paper and with the **Me$_2$DAB** backbone to the rear (Figure 1). When viewing the *cis*-PtA_2**G**$_2$ complex from the **G** coordination side, a line connecting the O6 atoms will be rotated (by an angle <90°) clockwise (ΛHT) or counterclockwise (ΔHT) in order to be aligned with the perpendicular to the coordination plane.[47] Each HT atropisomer is C_2 symmetrical and has one H8 signal in (*S,R,R,S*)- or (*R,S,S,R*)-**Me$_2$DAB**Pt**G**$_2$ complexes (Figure 1). It should be noted that since we are starting with resolved **Me$_2$DAB** complexes, none of the **G** adducts in a given solution are enantiomers, even when **G** lacks a chiral substituent, e.g. 9-EtG. Only one HH atropisomer is possible for (*S,R,R,S*)- or (*R,S,S,R*)-**Me$_2$DAB**Pt**G**$_2$ complexes (Figure 1). Since the two H8's in each HH form are nonequivalent, two H8 signals are expected; thus, four H8 signals are expected when all three atropisomers are present.

An early preliminary NMR investigation of (*S,R,R,S*)- and (*R,S,S,R*)-**Me$_2$DAB**Pt(5′-GMP)$_2$ complexes[9] and a more recent study of analogues with the non-C_2-symmetrical (*S,S,S,R*)- and (*S,R,R,R*)-**Me$_2$DAB** ligands[6] demonstrated that the atropisomer distribution depends on the **Me$_2$DAB** configuration. The (*S,R,R,S*)- and (*R,S,S,R*)-**Me$_2$DAB**Pt(5′-GMP)$_2$ complexes had the distribution major HT > HH > minor HT, but the chirality of the major HT form was opposite for the two **Me$_2$DAB** chiralities.[9] We now recognize that **Me$_2$DAB** is a chirality-controlling chelate (**CCC**) ligand; other examples of such carrier ligands for platinum are under study in our laboratories. However, chirality control was not found in complexes with the non-C_2-symmetrical **Me$_2$DAB** ligands with secondary NH groups on the same side of the platinum coordination plane. For both (*S,S,S,R*)- and (*S,R,R,R*)-**Me$_2$DAB**Pt(5′-GMP)$_2$ systems, the ΔHT and ΛHT atropisomers had comparable stabilities and the HH atropisomers were almost undetectable.[6] If either phosphate−NH or O6−NH hydrogen bonding were a principal stabilizing factor, one of the two possible HH forms would be the major species formed since in each HH conformation two similar hydrogen bonds (phosphate-NH or O6−NH) are possible. These different results for these **Me$_2$DAB** complexes suggested that several factors other than NH hydrogen bonding probably contribute to the relative stability of the atropisomers.

Since previous studies with C_2-symmetrical **Me$_2$DAB**Pt moieties were limited in scope, we have now employed both NMR and CD (circular dichroism) spectroscopy to study (*S,R,R,S*)- and (*R,S,S,R*)-**Me$_2$DAB**Pt**G**$_2$ complexes with **G** = 5′-GMP, 3′-GMP, and 9-EtG.[48] Different **G** moieties were chosen in order to investigate the effect on the conformational equilibrium of the presence of a phosphate group, the position of a phosphate group, and the absence of a sugar−phosphate group. We also examined the effect of a sugar with the (*S,R,R,S*)-**Me$_2$DAB**Pt**G**$_2$ (**G** = Guo and 1-MeGuo)[48] complexes.

Experimental Section

Preparation of Me$_2$DABPtG$_2$ Complexes. Typically, a stock **G** solution (~20−30 mM in D_2O, **G** from commercial sources) was prepared at pH ~3 (adjusted with ~20 μL of a 10% DNO_3 with stirring); a lower pH (~1.6) was required to dissolve 9-EtG. An aliquot (0.55 mL) of this stock solution was then added to an NMR tube containing the required amount of **Me$_2$DAB**Pt$(NO_3)_2$ or **Me$_2$DAB**Pt$(SO_4)(H_2O)$, synthesized as described elsewhere.[6] The progress of the reaction at ambient temperature was monitored by ^{1}H NMR spectroscopy using the residual HOD peak as a reference; a typical reaction time was ~1−3 h, but the solution was kept for up to several days to ensure complete reaction. When necessary, the pH was adjusted to ~3 by adding a small amount of DNO_3 or NaOD; in some cases, a slight excess of **G** was present, but since the signals in the NMR spectrum were easily identified and the CD signals of **G** are weak, such solutions were often used in spectral studies. For the 2D NMR studies, a larger aliquot (1.1 mL) of the stock solution was added to an NMR tube. After complete reaction, the sample was lyophilized and redissolved in 99.96% D_2O (0.55 mL, final concentration ~40 mM in **G**).

NMR Spectroscopy. 2D data were collected on the GE GN 500 MHz or Omega 600 MHz spectrometers with a 5555.6 or 6666.67 Hz spectral window in both dimensions, respectively. All pulse sequences began with a 2.0−2.5 s water presaturation pulse.

The 2D ^{1}H−^{1}H phase-sensitive COSY[49] spectra were collected at 5 °C for (*S,R,R,S*)-**Me$_2$DAB**Pt(5′-GMP)$_2$ and [(*S,R,R,S*)-**Me$_2$DAB**Pt(1-MeGuo)$_2$]$^{2+}$ on the GE GN 500. A 512 × 2048 data matrix was collected with 64 scans per t_1 period. After four dummy scans, the initial presaturation pulse was followed by a 10 ms delay. The data were processed in a phase-sensitive States mode with Felix (Molecular Simulations, Inc.). A Gaussian filter with a 0.2 coefficient and a line broadening of 3 Hz was applied to the acquisition dimension and either a 30 or 45° phase shifted sine-squared function was applied to the 512 points in the evolution dimension, which was then zero-filled to 2048 points.

2D ^{1}H−^{1}H NOESY[50] experiments were performed at 5 °C by collecting a 512 × 2048 matrix with 64−128 scans per t_1, and a mixing time of 500 ms. Each block of data was preceded by four dummy scans. The data were processed in the phase-sensitive mode by applying exponential multiplication and an 80−90° shifted sine-squared function in the first and second dimension, respectively.

CD Spectroscopy. CD spectra of ~4 × 10^{-5} M solutions were recorded on a JASCO 600 spectropolarimeter at ambient temperature. To improve signal/noise, four spectra were acquired in succession and averaged.

Results

The ^{1}H NMR spectrum of (*S,R,R,S*)-**Me$_2$DAB**Pt$(D_2O)(SO_4)$ in D_2O at pH 3.3 had one set of signals from the two magnetically equivalent halves of **Me$_2$DAB** (a broad NH singlet at 6.15 ppm, a CH multiplet at 2.51 ppm, and NCH_3 and CCH_3 doublets at 2.49 and 1.20 ppm, respectively). The spectrum was consistent with the presence of [(*S,R,R,S*)-**Me$_2$DAB**Pt$(D_2O)_2$]$^{2+}$ in solution. All **Me$_2$DAB**Pt**G**$_2$ samples had spectra with multiple H8 signals characteristic of atropisomers. In the pH ~1−3.5

(47) Williams, K. M.; Cerasino, L.; Intini, F. P.; Natile, G.; Marzilli, L. G. *Inorg. Chem.* **1998**, *37*, 5260.

(48) Abbreviations: 5′-GMP, guanosine 5′-monophosphate; 3′-GMP, guanosine 3′-monophosphate; Guo, guanosine; 1-MeGuo, 1-methylguanosine; 9-EtG, 9-ethylguanine.

(49) Bax, A.; Freeman, R.; Morris, G. *J. Magn. Reson.* **1981**, *42*, 164.

(50) Kumar, A.; Ernst, R. R.; Wüthrich, K. *Biochem. Biophys. Res. Commun.* **1980**, *95*, 1.

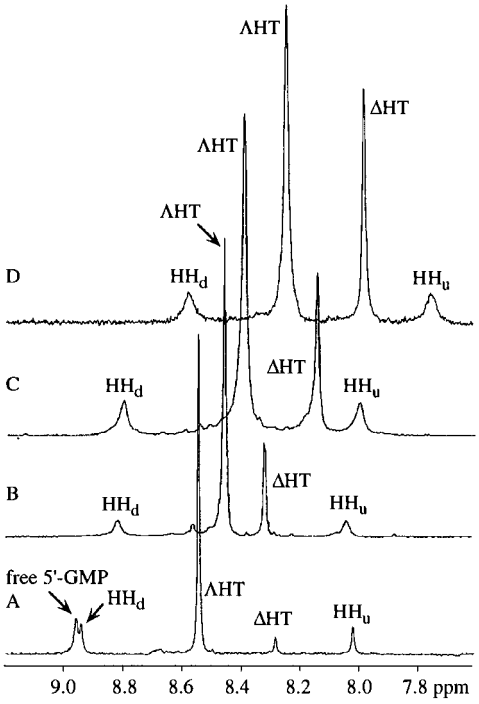

Figure 2. H8 region of the ^{1}H NMR spectra (5 °C) of (*S,R,R,S*)-**Me$_2$DAB**Pt**G**$_2$ for **G** = 5′-GMP (A); 3′-GMP (B); 1-MeGuo (C); and 9-EtG (D).

range, the H8 signals did not exhibit downfield shifts, an indication that Pt was bound to the N7 of **G**.

(*S,R,R,S*)-Me$_2$DABPtG$_2$ Complexes (G = 5′-GMP, 3′-GMP, 1-MeGuo, and 9-EtG). General Observations. Atropisomers expected for bis adducts of the type (*S,R,R,S*)-**Me$_2$DAB**Pt**G**$_2$ were discussed above (see Figure 1). Each C_2-symmetrical HT atropisomer has one set of ^{1}H NMR signals. For the HH atropisomer, two different H8 signals and two signals from the NCH_3, NH, CCH_3 and CH groups of (*S,R,R,S*)-**Me$_2$DAB** are possible. Four (*S,R,R,S*)-**Me$_2$DAB**Pt**G**$_2$ H8 signals were observed for each sample (Figure 2); these signals appeared upfield to the free **G** signals (due to the low pH of the solution), usually within 10 min. The reaction was considered complete when an added excess of **G** produced no new H8 signals.

A NOESY/EXSY experiment was performed for several samples using a standard protocol at the same temperature and mixing time. In all NOESY/EXSY spectra of **Me$_2$DAB**Pt**G**$_2$ complexes, there were exchange cross-peaks in the H8 and NH regions, indicating that the three atropisomers were interconverting (Figure 3 and Supporting Information). The line widths and the cross-peaks give a rough indication of the relative dependence of the rotation rates on the nature of the **G** ligand.

G = 5′-GMP. The ^{1}H NMR spectrum (20 °C) of a solution containing [(*S,R,R,S*)-**Me$_2$DAB**Pt$(D_2O)_2]^{2+}$ and 5′-GMP contained six new H8 peaks 10 min after mixing. Two transient signals of similar size were assigned to the two [(*S,R,R,S*)-**Me$_2$DAB**Pt(D_2O)(5′-GMP)]$^+$ intermediates. The remaining four H8 signals were attributed to the three (*S,R,R,S*)-**Me$_2$DAB**Pt-$(5′\text{-GMP})_2$ atropisomers (Figure 2). The shifts of these H8 signals showed little temperature dependence; in general, the H8 resonances shifted upfield by < 0.08 ppm, and there was no significant change in line widths from 5 to 20 °C.

In the 5 °C spectrum (Table 1), two well-separated signals of equal intensity at 8.02 and 8.94 ppm, designated HH$_u$ and HH$_d$, respectively, were from the HH atropisomer; the other two signals, at 8.28 and 8.54 ppm, were from the HT minor and HT major species, respectively. This pattern of H8 signals

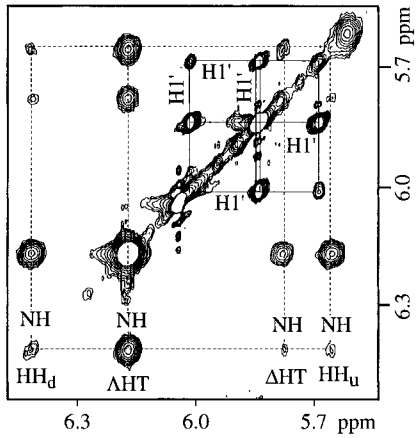

Figure 3. NH and H1′ regions of the NOESY/EXSY spectrum (5 °C) of (*S,R,R,S*)-**Me$_2$DAB**Pt$(5′\text{-GMP})_2$. The NH signals are labeled by conformation, and dashed lines connect the exchange network. The H1′ signal exchange network is connected with solid lines.

(one dominant and downfield HT H8) is typical of all **Me$_2$DAB**Pt**G**$_2$ species studied here. The atropisomer ratio was 16.3:1.0:3.6 for ΛHT major:ΔHT minor:HH species. The determination of the Λ and Δ conformations is discussed below. The smaller population of the ΔHT atropisomer than that of the HH atropisomer is unique to the 5′-GMP adduct; in analogous (*S,R,R,S*)-**Me$_2$DAB**Pt**G**$_2$ adducts, the HH conformer was least abundant.

The 5.5−6.5 ppm region contained four NH resonances that were readily assigned by their relative intensities to the three atropisomers (Table 1). The NOESY/EXSY spectrum showed exchange cross-peaks between the NH resonances as well as between the H1′ signals (Figure 3). With increasing temperature, the NH resonances exhibited only a small linear temperature-dependent shift downfield.

From the H8-**Me$_2$DAB** NOESY cross-peaks, the absolute conformation of the two HT atropisomers can be determined. For the major HT atropisomer, the H8 signal had NOE cross-peaks to the NCH_3 and NH signals; the latter signals had cross-peaks allowing assignment of the remaining **Me$_2$DAB** signals (Table 1, Supporting Information). The relative ratio of 1.73 for these cross-peak volumes [(H8−NH × 3)/(H8−NCH_3), Table 1] demonstrates that the H8 atoms in this HT adduct are close to NH.[6,9] From the known *S,R,R,S* chirality of **Me$_2$DAB**, this atropisomer has the ΛHT conformation, which potentially could be stabilized by two phosphate−NH(**Me$_2$DAB**) hydrogen bonds. The other HT adduct must be the ΔHT atropisomer. Two O6−NH hydrogen bonds are possible for this ΔHT atropisomer.

G = 3′-GMP. As described above for the 5′-GMP system, six H8 signals were readily attributed to the three (*S,R,R,S*)-**Me$_2$DAB**Pt$(3′\text{-GMP})_2$ atropisomers and the two [(*S,R,R,S*)-**Me$_2$DAB**Pt(D_2O)(3′-GMP)]$^+$ intermediates. However, the H8 signals for (*S,R,R,S*)-**Me$_2$DAB**Pt$(3′\text{-GMP})_2$ and all other (*S,R,R,S*)-**Me$_2$DAB**Pt**G**$_2$ species were broader than for (*S,R,R,S*)-**Me$_2$DAB**Pt$(5′\text{-GMP})_2$. The atropisomeric ratio for ΛHT major:ΔHT minor:HH was 4.4:1.3:1. The four NH signals (Table 1) from the three atropisomers showed little temperature dependence and had exchange cross-peaks between them in the 5 °C NOESY/EXSY spectrum.

For the major HT atropisomer, the H8 signal had cross-peaks to its NCH_3 and NH signals (Table 1 and Supporting Information). The finding that the volume of the H8−NH cross-peak was about twice (after normalization) that of the H8−NCH_3 cross-peak defined the ΛHT conformation (Table 1). These NH and NCH_3 signals had NOE cross-peaks to CCH_3 and CH

Table 1. ^{1}H NMR Signals (ppm) and Relative Volumes[a] of NOE Cross-Peaks between H8 and **Me$_2$DAB** NH and NCH_3 Signals in the NOESY/EXSY Spectra of **Me$_2$DAB**Pt**G**$_2$ Samples

G (signal)	δH8	δNH	δNCH_3	δCCH_3	δCH	δH1′	relative volume
			(*S,R,R,S*)-**Me$_2$DAB**Pt**G**$_2$				
5′-GMP HHu	8.02	5.65	*b*	*b*	*b*	5.68/6.02	*b*
5′-GMP ΔHT	8.28	5.78	*b*	*b*	*b*	5.84	*b*
5′-GMP ΛHT	8.54	6.18	2.29	1.21	2.74	5.84	1.73
5′-GMP HHd	8.94	6.43	*b*	*b*	*b*	5.68/6.02	*b*
3′-GMP HHu	8.03	5.76/6.19	*b*	*b*	*b*	*b*	*b*
3′-GMP ΔHT	8.31	5.81	2.35	1.25	2.82	5.87	0.13
3′-GMP ΛHT	8.45	6.08	2.29	1.23	2.76	5.87	2.10
3′-GMP HHd	8.82	5.76/6.19	*b*	*b*	*b*	*b*	*b*
1-MeGuo HHu	7.99	5.78/6.15	*b*	*b*	*b*	*b*	*b*
1-MeGuo ΔHT	8.14	5.70	2.32	1.26	2.85	5.81	0.0
1-MeGuo ΛHT	8.38	6.09	2.26	1.24	2.76	5.81	∞
1-MeGuo HHd	8.78	5.78/6.15	*b*	*b*	*b*	*b*	*b*
			(*R,S,S,R*)-**Me$_2$DAB**Pt(3′-GMP)$_2$				
HHu	8.09	5.86/6.13	*b*	*b*	*b*	*b*	*b*
ΛHT	8.27	5.82	2.37	1.26	2.84	5.86	0.0
ΔHT	8.56	6.13	2.36	1.26	2.78	5.93	3.3
HHd	8.81	5.86/6.13	*b*	*b*	*b*	*b*	*b*

[a] Relative volume was calculated by multiplying the volume of the H8/NH cross-peak by three and then dividing by the volume of the H8/NCH_3 cross-peak. [b] Not assigned.

signals (Table 1). For the minor HT atropisomer, the ΔHT conformation was defined by the H8−NCH_3 NOE cross-peak at 8.31−2.35 ppm (Supporting Information).

G = 1-MeGuo. The H8 signals of [(*S,R,R,S*)-**Me$_2$DAB**Pt(1-MeGuo)$_2$]$^{2+}$ are broad at 25 °C. By integration of the sharper H8 resonances at 5 °C, the ΛHT major:ΔHT minor:HH ratio was ∼3.8:1.6:1. For the major HT atropisomer, the H8 signal had a NOESY cross-peak to the NH signal (Supporting Information). The NH signal had a cross-peak to the NCH_3 signal at 2.26 ppm. These NCH_3 and NH signals had cross-peaks to the CCH_3 and CH signals at 1.24 and 2.76 ppm, respectively (these (*S,R,R,S*)-**Me$_2$DAB** signal assignments were confirmed by COSY data) (Table 1). Thus, the most stable atropisomer was again found to have the ΛHT conformation.

The H8 signal of the minor HT atropisomer had an H8−NCH_3 cross-peak, but no H8−NH cross-peak, results consistent with the ΔHT conformation (Table 1 and Supporting Information). The NCH_3 signal had a cross-peak to the NH signal at 5.70 ppm. Assignment of the ΔHT atropisomer signals was completed through numerous NOE cross-peaks involving NH, NCH_3, CCH_3, and CH signals (Table 1).

G = Guo. For this complex, the conformation of the dominant HT atropisomer was determined by CD spectroscopy (see below). Integration gave 3.0:1.5:1 for ΛHT major (8.40 ppm):ΔHT minor (8.18 ppm):HH (8.00 and 8.77 ppm). There was only one H1′ signal (at 5.83 ppm).

G = 9-EtG. Only two large broad HT H8 signals are present at 20 °C in the ^{1}H NMR spectrum of a solution containing [(*S,R,R,S*)-**Me$_2$DAB**Pt(9-EtG)$_2$]$^{2+}$. At 5 °C, these H8 signals sharpened to almost half their former width, and two additional HH H8 signals of equal intensity emerged (Figure 2); integration gave 2.9:1.5:1 for ΛHT major (8.22 ppm):ΔHT minor (7.96 ppm):HH (7.74 and 8.55 ppm); the HT conformation was determined by CD spectroscopy (next paragraph) because the dynamic motion precluded the determination of cross-peak intensities. Other signals identified include NH for ΛHT (6.01 ppm), ΔHT (5.71 ppm), HH (5.82/6.12 ppm); NCH_3 for ΛHT (2.30 ppm), ΔHT (2.35 ppm); CH for ΛHT (2.78 ppm), ΔHT (2.86 ppm); and CCH_3 for ΛHT (1.29 ppm), ΔHT (1.29 ppm). The Et signals were not resolved for each atropisomer and appeared at 4.06 (CH_2) and 1.35 (CH_3) ppm.

***(R,S,S,R)*-Me$_2$DABPtG$_2$ Complexes (G = 5′-GMP, 3′-GMP, and 9-EtG). G = 3′-GMP.** The ^{1}H NMR spectrum for this complex has the characteristic four H8 peaks (Table 1 and Supporting Information). In the 2D NOESY spectrum, the relative volume ratio for the major HT atropisomer is >1, indicating that this is a ΔHT rotamer (Table 1). All signals were readily assigned as above. A 1D integration of the H8 region showed an atropisomeric ratio of 9.8:1.8:1 for ΔHTmajor:ΛHT minor:HH. There are exchange cross-peaks between each NH signal. The connectivities between all four H8 signals (Supporting Information) demonstrate that all three possible atropisomers are in chemical exchange.

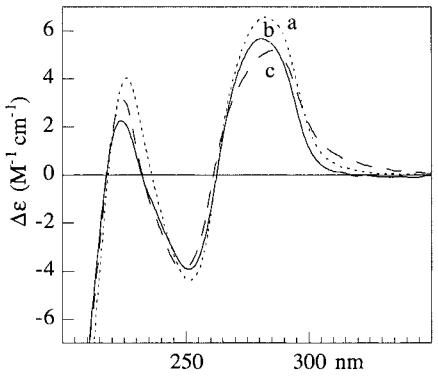

Figure 4. CD spectra of (a) (*S,R,R,S*)-**Me$_2$DAB**Pt(5′-GMP)$_2$, (b) (*S,R,R,S*)-**Me$_2$DAB**Pt(3′-GMP)$_2$, and (c) [(*S,R,R,S*)-**Me$_2$DAB**Pt(9-EtG)$_2$]$^{2+}$ at pH 3.

G = 5′-GMP. The ^{1}H NMR spectrum (20 °C) of the (*R,S,S,R*)-**Me$_2$DAB**Pt(5′-GMP)$_2$ solution at pH 3 has four H8 signals. Two signals of equal intensity at 8.09 and 8.95 ppm were from the HH atropisomer; the other two, at 8.28 and 8.74 ppm, were from the HT minor and HT major species, respectively. The atropisomer ratio was 10.3:1.0:2.8 for ΔHT major:ΛHT minor:HH species. Thus, again the minor HT form is less favored than the HH form when **G** = 5′-GMP.

G = 9-EtG. The ^{1}H NMR spectrum of the [(*R,S,S,R*)-**Me$_2$DAB**Pt(9-EtG)$_2$]$^{2+}$ solution is identical to that of [(*S,R,R,S*)-**Me$_2$DAB**Pt(9-EtG)$_2$]$^{2+}$, as expected for true enantiomers.

CD Spectra of (*S,R,R,S*)-Me$_2$DABPtG$_2$ and (*R,S,S,R*)-Me$_2$DABPtG$_2$. The CD spectra of (*S,R,R,S*)-**Me$_2$DAB**Pt**G**$_2$ complexes (Figure 4 and Supporting Information) all have the same shape, i.e., positive peaks at ∼285 and 230 nm and negative peaks at 250 and 210 nm. Since all the 2D NMR studies

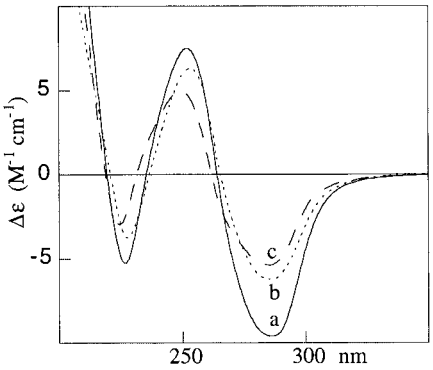

Figure 5. CD spectra of (a) (*R*,*S*,*S*,*R*)-**Me$_2$DAB**Pt(3′-GMP)$_2$, (b) (*R*,*S*,*S*,*R*)-**Me$_2$DAB**Pt(5′-GMP)$_2$, and (c) [(*R*,*S*,*S*,*R*)-**Me$_2$DAB**Pt(9-EtG)$_2$]$^{2+}$ at pH 3.

showed the dominant atropisomer was ΛHT, this type of CD signal is designated as Λ. Since (*S*,*R*,*R*,*S*)-**Me$_2$DAB**Pt**G**$_2$ (**G** = 9-EtG and Guo) have this Λ CD spectrum and since the magnitude of the signals are similar for all these (*S*,*R*,*R*,*S*)-**Me$_2$DAB**Pt**G**$_2$ complexes, we conclude that the major atropisomer is the ΛHT rotamer in all cases. We shall make a stronger case for the chirality of the HT conformer dictating the sign of the CD in the Discussion.

The negative peaks at 285 and 230 nm and positive peaks at 250 and 210 nm in the CD spectra of (*R*,*S*,*S*,*R*)-**Me$_2$DAB**Pt**G**$_2$ complexes (Figure 5) have signs opposite to those of the corresponding peaks in the (*S*,*R*,*R*,*S*)-**Me$_2$DAB**Pt**G**$_2$ CD spectra. Since from the 2D NMR study the dominant atropisomer for (*R*,*S*,*S*,*R*)-**Me$_2$DAB**Pt(3′-GMP)$_2$ is a ΔHT rotamer, this type of CD signal is designated as Δ. The NMR and CD results are consistent and were used to assign the conformations of the other (*R*,*S*,*S*,*R*)-**Me$_2$DAB**Pt**G**$_2$ complexes. Our hypothesis that the chirality of the HT conformer dictates the sign of the CD is supported by the data since the CD spectra of (*S*,*R*,*R*,*S*)-**Me$_2$DAB**Pt**G**$_2$ and (*R*,*S*,*S*,*R*)-**Me$_2$DAB**Pt**G**$_2$ are opposite in sign, and these complexes have major HT conformers with opposite chiralities as determined by NMR methods.

Discussion

Our research program with analogues of cisplatin containing **CCC** ligands was designed to understand how the dynamic motion and conformation of Pt adducts with nucleic acids and their constituents are influenced by interligand interactions with the amine ligands. The specific goals of the present study were to investigate the factors that influence the stability of (*S*,*R*,*R*,*S*)- and (*R*,*S*,*S*,*R*)-**Me$_2$DAB**Pt**G**$_2$ atropisomers. The experiments conducted were designed to assess potential hydrogen-bonding interactions, steric interactions, and possible intramolecular phosphate interactions by comparing the spectral characteristics and atropisomer distributions of several **Me$_2$DAB**Pt**G**$_2$ species. The NMR spectra of all such species provide evidence for the presence of all three possible atropisomers and a similar pattern of chemical shifts. Since one HT atropisomer dominated, we used this system to place the interpretation of CD signals of *cis*-PtA$_2$**G**$_2$ compounds on a firmer foundation.

Inherent purine stacking forces (dipole interactions) drive nonbridged **G** moieties to orient in an HT arrangement, an established phenomenon both in solution state[6,9,36,39] and crystallographic studies.[19,36,51−54] In the case of the (*N*,*N*,*N*′,*N*′-tetramethylethylenediamine)Pt(Guo)$_2$ complex, where the bulky tertiary amine groups cannot form hydrogen bonds,[36] the only atropisomers observed have HT conformations; perhaps in this case HH conformers are sterically disfavored. The two HT conformers are equally favored in solution, but the ΔHT crystallized and was characterized by X-ray crystallography.[37] In the less hindered systems, it is not possible to assess the atropisomer distribution. In the solid state, the ΔHT form dominates almost invariably.[19,36,51−54]

Chart 2. Sketches of the Rotamers of (*S*,*R*,*R*,*S*)- and (*R*,*S*,*S*,*R*)-**Me$_2$DAB**Pt**G**$_2$ with Left-Handed and Right-Handed Tilt, Respectively

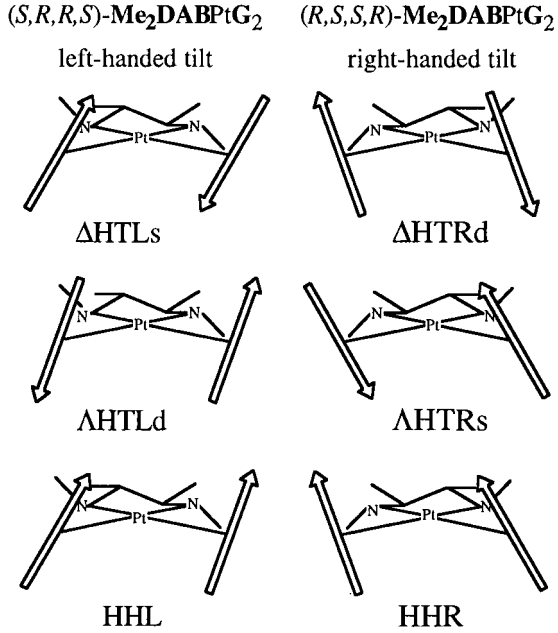

In the solid state, the ΔHT forms are observed exclusively, and these ΔHT forms cluster into two groups differing in the degree and direction of the tilt;[55] i.e., the bases can have either a left-handed (L) or a right-handed (R) tilt, illustrated for (*S*,*R*,*R*,*S*)- and (*R*,*S*,*S*,*R*)-**Me$_2$DAB**Pt**G**$_2$ in Chart 2. Relative to the average H8 signal, a lesser tilt gives less shielding and hence a deshielded (d) H8 signal, and the greater tilt gives a shielded (s) H8 signal. In theory, three sets of two variables lead to eight (2^3) possible forms, but computations indicate that there are only four stable HT forms, as follows: ΔHTLs, ΔHTRd, ΛHTLd, and ΛHTRs.[55] The consequences of this tilting on the NMR spectra and on the CD spectra of complexes have been analyzed. In addition to the NMR analysis relating tilting to shielding and deshielding of **G** H8,[55] it has also been suggested that such differences in tilting can lead to different signs in the CD spectra of such complexes.[56,57] We return to this latter suggestion below since other interpretations have also been advanced to explain the CD spectra.

Like every other **Me$_2$DAB**Pt**G**$_2$ system, [**Me$_2$DAB**Pt(9-EtG)$_2$]$^{2+}$, has a major HT atropisomer with a downfield H8 signal and a minor HT atropisomer with an upfield H8 signal. Thus, even with its very simple N9 substituent, this system is

(51) Miller, S. K.; van der Veer, D. G.; Marzilli, L. G. *J. Am. Chem. Soc.* **1985**, *107*, 1048.
(52) Marzilli, L. G.; Chalilpoyil, P.; Chiang, C. C.; Kistenmacher, T. J. *J. Am. Chem. Soc.* **1980**, *102*, 2480.
(53) Orbell, J. D.; Taylor, M. R.; Birch, S. L.; Lawton, S. E.; Vilkins, L. M.; Keefe, L. J. *Inorg. Chim. Acta* **1988**, *152*, 125.
(54) Barnham, K. J.; Bauer, C. J.; Djuran, M. I.; Mazid, M. A.; Rau, T.; Sadler, P. J. *Inorg. Chem.* **1995**, *34*, 2826.
(55) Kozelka, J.; Fouchet, M.; Chottard, J. *Eur. J. Biochem.* **1992**, *205*, 895.
(56) Gullotti, M.; Pacchioni, G.; Pasini, A.; Ugo, R. *Inorg. Chem.* **1982**, *21*, 2006.
(57) Pasini, A.; De Giacomo, L. *Inorg. Chim. Acta* **1996**, *248*, 225.

representative. Several factors could influence this shift relationship. However, a likely interpretation is that the major atropisomer has a lesser tilt and the minor atropisomer has a greater tilt since a shift difference of ~0.3 ppm was predicted for these differently tilted forms.[55] From our analysis of conformations, the minor forms could form **G** O6−NH hydrogen bonds. Such hydrogen bonding will increase the degree of tilt. For example, the left-handed tilted ΔHTLs form for (*S,R,R,S*)-**Me$_2$DAB**Pt**G**$_2$ (Chart 2) would allow **G** O6 hydrogen bonding to the NH's. Since the 9-EtG N9 substituent is not chiral, the minor atropisomers for the two different **Me$_2$DAB** configurations are exact enantiomers. We classify the minor forms of the (*S,R,R,S*)- and (*R,S,S,R*)-**Me$_2$DAB**Pt(9-EtG)$_2$ complexes as ΔHTLs and ΛHTRs, respectively. By the process of elimination combined with the observation that the minor and major HT forms with each **Me$_2$DAB** chirality have opposite chirality, the two major forms for (*S,R,R,S*)- and (*R,S,S,R*)-**Me$_2$DAB**Pt(9-EtG)$_2$ are ΛHTLd and ΔHTRd. These latter forms are reasonable since with these tilts the **G** O6's both avoid the bulky part of the **Me$_2$DAB** ligands. Thus, our analysis of the NMR data, considerations of hydrogen bonding and steric effects, the results of numerous X-ray structures, and finally computations all agree, and a consistent picture emerges.

An important consequence of the above analysis is that the two HT forms for a given **Me$_2$DAB** chirality have different degrees of tilt but the *same* tilt direction. Specifically, (*S,R,R,S*)-**Me$_2$DAB**Pt(9-EtG)$_2$ has two L HT forms, a ΛHTLd major form and a ΔHTLs minor form. From similar reasoning, the HH form has the same tilt direction as the major and minor forms, but one **G** is less tilted and one **G** more tilted. Such tilting not only minimizes steric interactions but it also provides an explanation for the dispersion of the H8 signals.

We can now analyze the longstanding interpretation of the origin of the CD signals.[56,57] It was stated that the sign of the CD depended on the tilt direction, and the opposite CD shapes indicated R vs L tilt. Our results suggest that the tilts of both the major and the minor HT forms of a given analogue are the same. Therefore, the sign of the CD signals would be the same if the interpretation is correct, and the CD signals would be of roughly opposite shape for the complexes with different **Me$_2$DAB** chirality. For (*S,R,R,S*)-**Me$_2$DAB**Pt**G**$_2$, the percentage of ΛHT for the 5′-GMP, 3′-GMP, and 9-EtG adducts is 78%, 66%, and 54%, respectively; the CD signal intensity at ~285 nm is 6.6, 5.7, and 5.2 M^{-1} cm^{-1}, respectively (Figure 4). For (*R,S,S,R*)-**Me$_2$DAB**Pt**G**$_2$, the percentage of ΔHT for the 3′-GMP, 5′-GMP, and 9-EtG adducts is 78%, 73%, and 54%, respectively; and the CD signal intensity at ~285 nm is −9.6, −6.2, and −5.4 M^{-1} cm^{-1}, respectively (Figure 5). The CD shapes are thus roughly opposite, apparently consistent with the tilt governing the sign. We do not accept the hypothesis that the CD shape is dictated by the tilt direction because CD intensity roughly correlates with the percentage of the major HT form. We hypothesize that the sign of the CD is dictated by the HT chirality. At present, there is no compelling experimental evidence with **Me$_2$DAB** complexes to distinguish the older literature hypothesis and our hypothesis. However, with the related **Bip** complexes we found that a statistical mixture of 25% ΔHT, 50% HH, and 25% ΛHT had almost no CD intensity.[44] With time, the CD intensity increased as the favored HT form became dominant. Above we concluded that all three forms have the same tilt direction. No large increase in CD intensity would have been observed if tilt direction determined the sign of the CD signal. Thus, we favor our analysis that the sign of the CD signal is more reflective of the Δ or Λ conformation of the HT form than of the tilt direction of the two **G** bases in the HT form.

We turn now to consider the role of the N9 group. Although there are variations in the atropisomer ratios, one HT atropisomer in all **Me$_2$DAB**Pt**G**$_2$ systems dominates in solution; this finding leads us to believe that the base−base interactions are major factors in determining the greater stability of the HT over the HH arrangement. Moreover, in the solid state, the HH atropisomers are rare and restricted to *cis*-PtA$_2$**G**$_2$ compounds with simple (nonsugar containing) **G**'s.[34,58] We reiterate the observations cited above that the ΔHT form was favored for the solid state. This finding encompasses a large number of compounds with different metal centers and different 6-oxopurine ligands containing D-ribose sugars.[19,36,51−54] The prevalence of the ΔHT form indicates that the sugar chirality (and hence the N9 substituent) does have some influence on conformation since the starting metal compounds were not chiral. We first consider here the 9-EtG and Guo derivatives. The N9 substituent in **Me$_2$DAB**Pt**G**$_2$ species is too small to interact with the diamine or with the N9 substituent of the cis **G**, but these N9 substituents can possibly interact with the *cis*-base. For these 9-EtG and Guo derivatives, the only other interligand interactions possible are the base−base and base−**Me$_2$DAB** interactions present in all **Me$_2$DAB**Pt**G**$_2$ species.

Models suggest that the 9-Et group cannot interact well with the *cis*-**G** base. Indeed, no separate Et ^{1}H NMR signals were observed for the different atropisomers. Furthermore, the larger D-ribose substituent has a relatively minor effect on atropisomer distribution in the Guo complex compared to the 9-EtG complex. This complex has only one H1′ signal and a CD signal similar to that of the 9-EtG complex. Thus, in these cases, it seems clear that the N9 substituent has no important interactions with other ligands. The presence of a 1-Me group in the 1-MeGuo complex also has relatively little effect. Since the favored HT rotamer [**Me$_2$DAB**Pt(9-EtG)$_2$]$^{2+}$ has no possibility of forming O6−NH hydrogen bonds, this observation suggests that O6−NH hydrogen bonding is not a very important factor influencing stability.

The ratio (ΔHT + ΛHT)/HH exhibits a remarkable trend; with only one exception, this ratio is nearly constant at ~4−6, regardless of the **Me$_2$DAB** configuration or the N9 substituent. The only exception is the (*R,S,S,R*)-**Me$_2$DAB**Pt(3′-GMP)$_2$ complex, for which the (ΔHT + ΛHT)/HH ratio is ~12. The ΔHT/ΛHT ratio of ~5 is not particularly unusual, suggesting that a large negative phosphate group substituent in this 3′-position is not important in the HT atropisomers, where the phosphate groups are quite distant. We suspect that the ratio of 12 might arise from unfavorable phosphate-phosphate interactions in the HH form. We do not have a clear understanding of this deviation, but in free energy terms the effect is small.

The most dramatic consistent difference from the pattern exhibited by the 9-EtG complex is found in the 5′-GMP complexes. Against the background of results now available for several **G**'s, the 5′-phosphate group clearly further stabilizes the favored major HT atropisomer over the minor HT atropisomer regardless of the ΔHT or ΛHT conformation. The 5′-phosphate group is positioned on the sugar such that it could interact with the cis **G** in any rotamer. Indeed, in the dominant ΛHT or ΔHT form of the C_2-symmetrical (*S,R,R,S*)- and (*R,S,S,R*)-**Me$_2$DAB**Pt(5′-GMP)$_2$ complexes, the phosphate groups are on the opposite side of the platinum coordination plane from each other but on the same side as the respective cis NH of the

(58) Schöllhorn, H.; Raudaschl-Sieber, G.; Müller, G.; Thewalt, U.; Lippert, B. *J. Am. Chem. Soc.* **1985**, *107*, 5932.

diamine; thus, the current results suggest that the formation of two phosphate−NH(**Me$_2$DAB**) hydrogen bonds could be a contributing factor in further stabilizing the dominant atropisomer since the 5′-phosphate group is positioned to form these NH(**Me$_2$DAB**) hydrogen bonds.

In the present study of several complexes with C_2-symmetrical **CCC** ligands, the 5′-GMP complexes have a relatively high amount of the HH atropisomer compared to the minor HT rotamer; unlike the case for other **G**'s, one phosphate−NH hydrogen bond is possible for the 5′-GMP HH forms. Such a phosphate−NH hydrogen bond could be the stabilizing factor accounting for the relatively high percentage of the HH form. If we use the preferred tilt for each **Me$_2$DAB** configuration, it is possible to construct HH models for the 5′-GMP complexes in which there are two NH hydrogen bonds, one to **G** O6 and one to phosphate. Although in these models the tilt direction would be the same as for the HT forms for that **Me$_2$DAB** configuration, the degree of tilt will be different for the two bases. It is likely that the **G** which cannot form a **G** O6−NH(**Me$_2$DAB**) hydrogen bond will have a lesser tilt (possibly even in the other direction) than in the respective major HT form, whereas the other **G** will have as great if not greater tilt than in the respective minor HT form. In such models, steric clashes of the *N*-methyl group of **Me$_2$DAB** and **G** base are avoided. Similar HH structures are possible with the other **G**'s used in this study, but there could be no stabilizing phosphate−NH hydrogen bond. The formation of only the one probably weak **G** O6−NH(**Me$_2$DAB**) hydrogen bond explains why the HH form is the least stable atropisomer in all cases but 5′-GMP. For the non-C_2-symmetrical **Me$_2$DAB** complexes, the presence of two hydrogen bonds of the same type in either possible HH form would lead to opposite directions of base tilt in both cases. Thus the order of HH stability, 5′-GMP (C_2-symmetrical **Me$_2$DAB**) > other **G** (C_2-symmetrical **Me$_2$DAB**) > 5′-GMP (non-C_2-symmetrical **Me$_2$DAB**), can be rationalized. This interpretation is also in keeping with the rather downfield shift of the HH$_d$ **G** H8 signals in both 5′-GMP HH complexes studied here. The hydrogen-bonded phosphate group of the less tilted 5′-GMP is close to the **G** H8 of this nucleotide.

Conclusions

On the basis of our results with the C_2-symmetrical **Me$_2$DAB** complexes, we can reach general conclusions about complexes with chirality-controlling chelate (**CCC**) ligands. In such complexes, the **CCC** ligand determines the L or R tilt and, within each of these, determines which atropisomers (Δ or Λ) will have small (d) and which will have large (s) tilts. The HT form with the lesser tilt dominates over that with the greater tilt. Thus, the ΔHTRd form is more stable than the ΛHTRs form, and ΛHTLd is more stable than ΔHTLs. This observation is independent of the N9 substituent, but the relative preference of the Λ vs Δ HT forms with the same tilt is modulated by the N9 substituent. Also, the **CCC** ligand configuration determines the tilt direction (R vs L) and thus the chirality (Λ or Δ) of the major HT form.

Complexes of the type (**CCC**)Pt**G**$_2$ with C_2-symmetrical **CCC** ligands do form minor amounts of HH complexes. These rare species have one **G** base with a lesser tilt and one with a greater tilt; the latter has the same tilt direction as the Δ and Λ HT forms for that **CCC** configuration. **CCC** NH to **G** O6 hydrogen bonding appears to help stabilize the minor forms (ΛHTR and ΔHTL) and the HH forms of such (**CCC**)Pt**G**$_2$ complexes. An additional hydrogen-bonding interaction between a 5′-phosphate and a **CCC** NH helps to stabilize the HH form of (**CCC**)Pt(5′-GMP)$_2$ complexes.

Acknowledgment. This work was supported by NIH Grant GM 29222 (to L.G.M.) and NATO CRG. 950376 (to L.G.M. and G.N.), and by MURST (Contribution 40%), CNR, and EC (COST Chemistry project D8/0012/97 (to G.N.).

Supporting Information Available: Figures of selected regions of the NOESY/EXSY spectra of **Me$_2$DAB**Pt**G**$_2$ complexes; H8 ^{1}H NMR signals of (*R*,*S*,*S*,*R*)-**Me$_2$DAB**Pt(3′-GMP)$_2$ at pH 3; and CD spectrum of [(*S*,*R*,*R*,*S*)-**Me$_2$DAB**Pt(Guo)$_2$]$^{2+}$ at pH 3 (10 pages). See any current masthead page for ordering information and Internet access instructions.

IC980843F